First Simultaneous Acceleration of Multiple Charge States of Heavy Ion Beams in a Large-Scale Superconducting Linear Accelerator

P. N. Ostroumov, K. Fukushima, T. Maruta, A. S. Plastun, J. Wei, T. Zhang, and Q. Zhao
Facility for Rare Isotope Beams, Michigan State University, East Lansing, Michigan 48824, USA

(Received 17 December 2020; accepted 22 February 2021; published 17 March 2021)

Experimental studies of the simultaneous acceleration of three-charge-state $^{129}Xe^{49+,50+,51+}$ beam from 17 to 180 MeV/nucleon in a superconducting linear accelerator are presented. The beam parameters for each individual- and multiple-charge-state beam were measured and compared with the particle tracking simulations. Detailed measurements were performed to characterize the multiple-charge-state beam's recombination after a second-order achromat and isopath 180° bending system. As a result of the recombination of three charge states in the six-dimensional phase space, the xenon beam intensity was increased by 2.5-fold compared to the single-charge-state beam. The results presented in the Letter fully validate the possibility to produce and utilize high-quality multiple-charge-state heavy-ion beams in a large-scale superconducting linac to increase the available beam power on an isotope production target.

DOI: 10.1103/PhysRevLett.126.114801

Introduction.—Charge stripping is required to boost the charge-to-mass ratio q/A of heavy-ion beams for economic acceleration to higher energies. In general, stripping of a heavy-ion beam produces multiple charge states. The charge distribution is approximately described by the Gaussian function centered on the mean charge state. The mean and the spread of the charge state distribution are functions of ion beam velocity, ion atomic mass, stripper material, and its thickness. The physics of ion-matter interaction related to the strippers is well described in the recent review article [1]. As mentioned in Ref. [1], the stripping of 17 MeV/nucleon uranium beam in a liquid lithium film yields just 22% of initial intensity in the main charge state 78+. Therefore, the driver linac of the Facility for Rare Isotope Beam (FRIB) [2] was designed to accept multiple charge states after the stripping and to simultaneously accelerate them to deliver a 400 kW beam on the isotope production target. The charge stripper's location in the FRIB driver linac was optimized to minimize the total accelerating voltage. The prestripper section of the linac can deliver beams at an energy range from 17 to 20 MeV/nucleon, depending on the ion's atomic mass.

The concept of multiple-charge-state heavy-ion beam acceleration was qualitatively discussed in the literature in the 1970s [3]. In the early 2000s, the acceleration of the multiple-charge-state uranium beam was demonstrated in a short section of a SC linac [4]. The theoretical description of the concept was reported earlier [5]. Later, this concept was adopted to design the FRIB project to achieve the required beam power on the production target [6].

The FRIB superconducting linac is being commissioned in stages, and recently, several ion species were accelerated up to 200 MeV/nucleon using available 278 SC resonators out of a total of 330 resonators. Recently, the three-charge-state xenon beam's simultaneous acceleration up to 180 MeV/u was successfully demonstrated. The charge state 27+ of the xenon beam produced by Electron Cyclotron Resonance Ion Source was selected for acceleration up to 17 MeV/nucleon to the stripper location. After the stripping, the charge state 50+ was selected for tuning the following rebunchers and magnetic optical system (MOS) designed for the recombination of multiple-charge-state beams in the six-dimensional phase space with minimal transverse and longitudinal effective emittance growth of the recombined beam. Detailed measurements were performed to characterize the multiple-charge-state beam's recombination after the MOS. These high accuracy bunch centroid measurements were possible thanks to the high sensitivity of beam position and phase monitors (BPPM) [7]. The transverse emittances of individual- and multiple-charge-state beams were measured and found in agreement with the expected phase space and well within the focusing channel's acceptance. As a result of proper recombination, the three-charge-state xenon beam's intensity was increased by a factor of 2.5 compared to the acceleration of the single-charge-state beam by simply opening the charge selection slits located in the high dispersion area of the MOS. With the same linac setting, the dual-charge-state $^{86}Kr^{33+,34+}$ beam was accelerated to 180 MeV/nucleon thanks to the average charge-to-mass ratio close to that of the $^{129}Xe^{50+}$ beam.

This Letter consists of three sections describing (1) the design concept of the magnetic optical system for recombination of a multiple-charge-state beam in the phase space, (2) the simultaneous acceleration of multiple charge states of heavy-ion beams, bunch centroid measurements, and

comparison with simulations, and (3) transverse rms emittance measurements and discussion.

Recombination of multiple-charge-state beam.—The simultaneous acceleration of multiple charge states of heavy-ion beams resolves two significant issues in the high-power accelerators: (1) obtaining high power of CW beams on the production target with limited available beam intensities from the ion source and (2) minimizing the beam power deposition on the charge selector slits after the stripper. The charge selector slits are required to intercept the unwanted charge states, which otherwise can cause uncontrolled beam losses along the linac. By selecting and accelerating multiple charge states, the beam losses on the selector slits are significantly reduced, which simplifies the radiation shielding of the charge selector to allow hands-on maintenance.

An advanced magnetic optical system (MOS) is required to achieve the acceleration of multiple charge states in the poststripper segment of the linac. In the FRIB linac, this MOS is realized as a 180° bending system with specific properties: (1) a section with a high dispersion capable of resolving different charge states spatially and intercepting the unwanted ones and (2) a section to recombine the bunch centroids of selected charge states of the ion beam in the six-dimensional phase space. The MOS was designed using the well-known TRANSPORT code [8]. The code uses coordinates $\vec{X} = (x, \theta, y, \varphi, l, \delta)$, where x, y are the particle transverse coordinates, θ, φ are the ratios of the particle's transverse momentum to the total momentum, l is the particle's longitudinal position with respect to the reference particle, δ is the particle's fractional momentum deviation from the reference particle. The layout of the MOS in the FRIB linac from the location of the stripper to the entrance of the next linac segment is shown in Fig. 1. The first rebuncher is necessary to minimize the momentum spread during the transport through the 180° bend. The second rebuncher provides matching to the following accelerating section. The transport of the particles through the MOS in linear approximation may be reduced to a matrix multiplication of an initial $\vec{X}(0)$ to final coordinates $\vec{X}(1)$:

$$\vec{X}(1) = R\vec{X}(0), \tag{1}$$

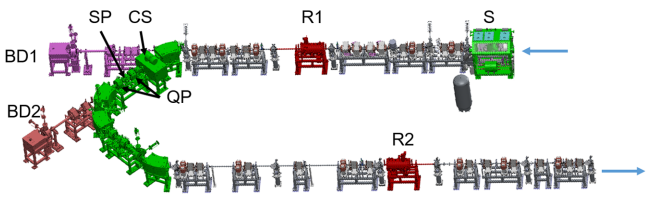

FIG. 1. The layout of the poststripper MOS of the FRIB linac. The blue arrows show the beam direction. *S*, stripper; *R*1 and *R*2, rebuncher 1 and 2; CS, charge selector; BD1 and BD2, beam dump 1 and 2; QP, quadrupole; SP, sextupole.

where R is 6×6 matrix. This formalism may be extended to the second order by introducing the second-order matrix T [8]:

$$X_i(1) = \sum_i R_{ij} X_j(0) + \sum_{j,k} T_{ijk} X_j(0) X_k(0)\,. \tag{2}$$

The MOS of the FRIB linac is composed of two identical parts placed with mirror symmetry. Each part includes two 45° bending magnets, two quadrupoles, a sextupole, and drift spaces. The charge states of the heavy-ion beam are separated horizontally after the first 45° bend, where the dispersion is high and equal to 1.5 m, and the beam is well focused horizontally. Using a pair of independently movable slits, single or multiple charge states can be selected for further transport and acceleration. The unwanted charge states are intercepted with the slits. The area is shielded to allow hands-on maintenance during the accelerator shutdown periods.

After the passage of the stripper, all charge states have equal average velocities and energies per nucleon. In constant magnetic fields, the particle charge qe and momentum p enter the equations of motion only as a ratio qe/p. Therefore, $\delta = \Delta p/p = -\Delta q/q$ and the path lengths of different charge states can be the same in an isopath system designed to provide equal path lengths for different momenta. The isopath condition can be met if the matrix elements of the MOS satisfy the condition $R_{51} = R_{52} = R_{53} = R_{54} = R_{56} = 0$ as follows from the expression (1). Because of the symmetry in the median plane, $R_{53} = R_{54} = 0$. The setting of the quadrupoles and drift spaces of the MOS was optimized to satisfy the conditions $R_{51} = R_{52} = R_{56} = 0$. The MOS has properties of an achromatic system, e.g., $R_{16} = R_{26} = 0$. For the multiple charge-state-beams, the major second-order contribution comes from an appreciable difference in charge states $\delta = \Delta q/q$. As a result, each charge state arrives at a different location in the horizontal and longitudinal phase space after the MOS. This can increase the effective emittance of the multiple-charge-state beam in both horizontal and longitudinal phase space. In the FRIB MOS, the strength of the sextupoles is optimized for $T_{166} = T_{266} = 0$ and to reduce the term T_{566}. As a result, there is no contribution of the charge dispersion into the effective transverse emittance growth of the multiple-charge-state beam. The dispersion function and rf bunch phase difference between the charge states in the section from the rebuncher 1 to the rebuncher 2 (see Fig. 1) were calculated using the second-order beam optics code and shown in Fig. 2. The term $T_{566} \sim (\Delta q/q)^2$ and not equal to zero; therefore, it results to a 5° deviation of the $^{129}Xe^{49+}$ and $^{129}Xe^{51+}$ centroids from the reference charge state 50+ as seen from Fig. 2. This deviation can be substantially reduced at the LS2 entrance using the second rebuncher, as shown in the following chapter.

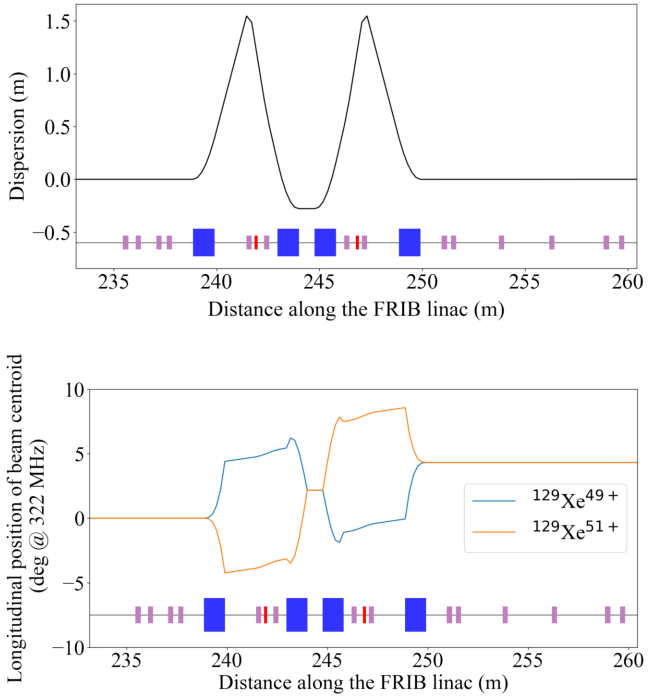

FIG. 2. The dispersion function (top) and the bunch's rf phase (bottom) along the MOS. Blue boxes correspond to magnetic dipoles, purple boxes to quadrupoles, red boxes to sextupoles.

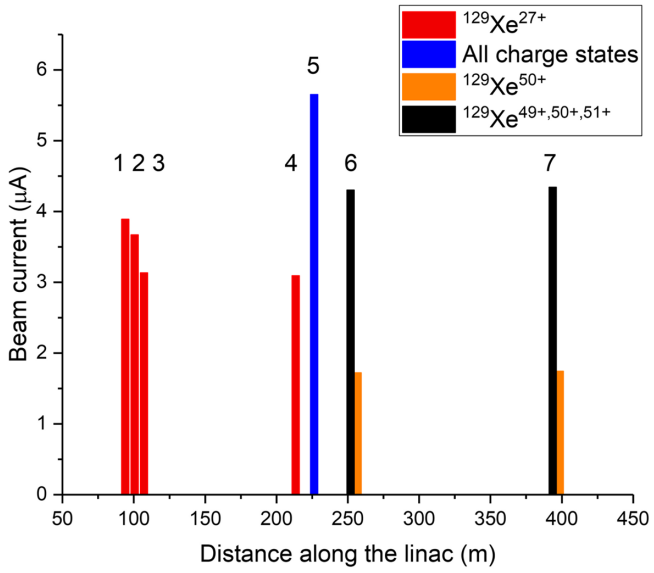

FIG. 3. Xenon beam current along the linac. Locations of BCMs are 1, upstream of the radio frequency quadrupole; 2, downstream of the radio frequency quadrupole; 3, entrance of the SC linac; 4, exit of the linac prestripper section; 5, after the stripper; 6, exit of the MOS and entrance of the LS2; 7, exit of the LS2.

Acceleration of multiple-charge-states beams.—Recently, the FRIB Linac Segment 2 (LS2), composed of 168 SC half-wave resonators (HWR), was commissioned, and a single-charge-state argon beam was accelerated up to 204 MeV/nucleon [9]. Recently, multiple-charge-state xenon and krypton beams were developed. The $^{129}Xe^{27+}$ beam was focused on the carbon foil stripper to produce a multiple-charge-state xenon beam. The main charge state 50+ after the stripper contains 32% of the initial intensity. The movable slits after the first 45° bending magnet were used to select a $^{129}Xe^{50+}$ beam. The settings of the prestripper section of the linac and charge selection features were discussed in our previous publication [10]. The linac components from the stripper to the beam dump at the end of LS2 were tuned for the transport and acceleration of $^{129}Xe^{50+}$ to 180 MeV/u with the synchronous phase ramped from −35° to −24° over 168 HWRs. After completing phase setting in all SC cavities, the beam centroid trajectory was corrected in the transverse phase planes with the orbit response matrix method [11]. The rms deviations of the beam centroid in 26 BPPMs were $\sigma_x = 0.8$ mm and $\sigma_y = 0.7$ mm. See Supplemental Material [12] for the measured beam centroid trajectory along the MOS and LS2. The transmission of the $^{129}Xe^{50+}$ beam after the charge selector to the beam dump located at the end of LS2 was measured with beam current monitors (BCM) [7] and was 100% within the 0.5% one-sigma accuracy of measurements. After completing the $^{129}Xe^{50+}$ beam tuning, the charge selector slits were opened to permit the transmission of three charge states $^{129}Xe^{49+,50+,51+}$, and a factor of 2.5 intensity increase of the 180 MeV/nucleon beam was measured. The transmission remained 100%, and no signals from beam halo monitors [7] were detected. The results of beam transmission measurements are shown in Fig. 3.

Until now, there was no opportunity to study the transport and recombination of bunched multiple-charge-state beams in the beam transport systems designed for a 180° bend. The proper beam recombination in the second-order achromatic system and correction of the beam center in the transverse phase space along the linac are the keys to minimizing the multiple-charge-state beam's effective emittance growth [3–5]. The charge selection slits were adjusted to select individual charge states 49+ and 51+ for acceleration in the linac with the same tune developed for the charge state 50+. Then, the bunch centroid positions x_c, y_c, z_c for each charge state 49+ and 51+ were measured by the BPPMs. Figures 4 show corresponding plots for the poststripper section of the linac. The plots presented in Figs. 4 are the relative measurements of the beam position and phase with respect to the reference charge state 50+. Therefore, the accuracy of measurements is a small fraction of millimeter and degree. One can see that the measured trajectories are well consistent with the simulations with the TRACK computer code [13], which tracks particle trajectories in three-dimensional electromagnetic fields and hence includes all higher-order optics terms. One can observe that the recombination of charge states 49+ and 51+ after the MOS in the longitudinal phase space is different from

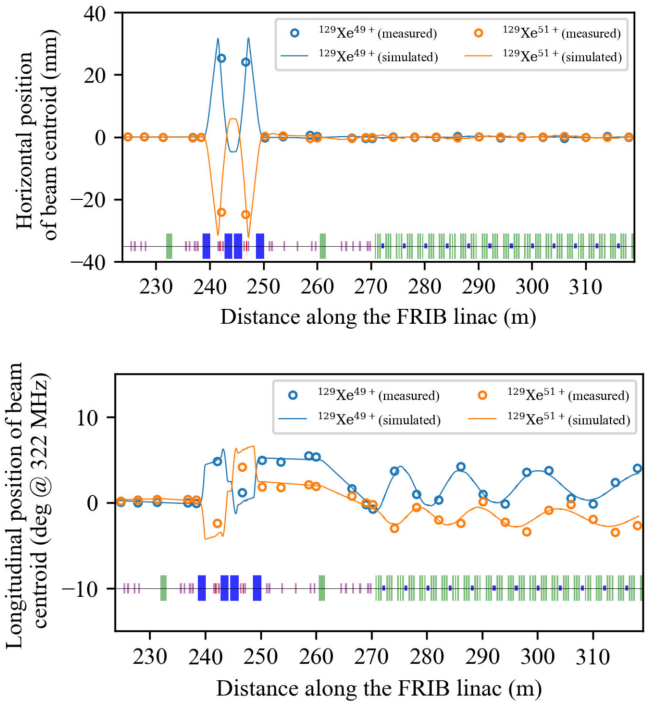

FIG. 4. The horizontal (top) and longitudinal positions (bottom) of the bunch centroid for charge states 49+ and 51+ with respect to the 50+ along the poststripper section of the linac. The position difference in the bottom plot is in degrees of 322 MHz, which is accelerating cavities' frequency in the LS2. Green boxes correspond to accelerating cavities, large blue boxes to magnetic dipoles, small blue boxes to SC solenoids with dipole correctors, and red boxes to quadrupoles.

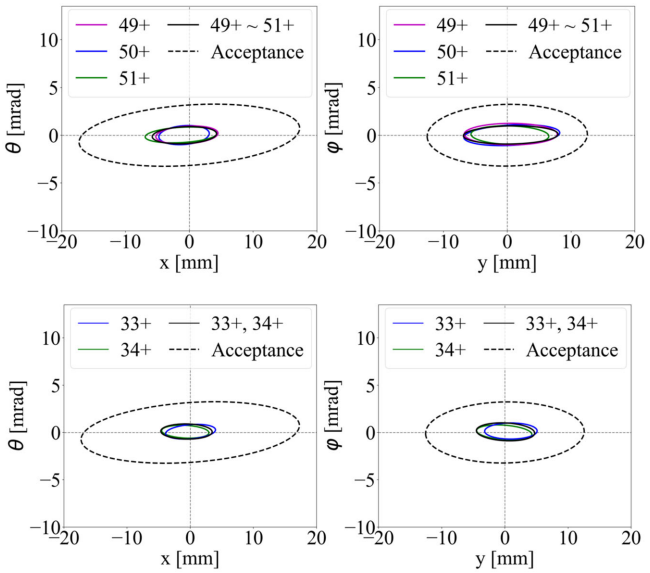

FIG. 5. 10σ emittances for the individual and multiple charge states and simulated acceptance of the following focusing channel for xenon (top) and krypton (bottom) beams.

Fig. 2 and caused by the contribution of higher-order terms. The remaining small differences between measurements and simulations could be related to the fact that the four 45° bending magnets are not fully identical. As a result, a trim coil in the third magnet was excited to align the beam center after the 180° bend. The rebuncher 2 minimizes the phase spread of the bunch centroid positions for different charge states at the entrance of LS2, as seen from the bottom plot in Fig. 4. The centroids of the charge states 49+ and 51+ oscillate around the reference charge state 50+ in the LS2 as follows from the concept of autophasing in an rf accelerator [5].

RMS emittance of multiple-charge-state beams.—In high intensity linacs, beam losses can be avoided if most particles occupy only a small fraction of the available acceptance. The transverse RMS emittance of the individual- and multiple-charge-state beams at the final energy of 180 MeV/nucleon were evaluated using the quadrupole scan method [10], which included beam profile measurements with wire scanners. The results are presented in the top plots in Fig. 5, which illustrates 10σ emittances for these four different cases for the xenon beam and the acceptance of the following linac section. The careful tuning of the xenon beam at the charge state 50+ resulted in a minimal effective emittance growth of the multiple-charge-state beam, less than 20% compared to the emittance of the single-charge-state beam. We observe slightly larger emittance in the vertical plane at this location, resulting from the emittance exchange between horizontal and vertical planes due to the strong coupling in the solenoidal focusing channel. The acceptance of the focusing channel is 57 and 123 times larger in the vertical and horizontal planes than the rms emittance of the multiple-charge-state xenon beam. Such a margin in the linac acceptance guarantees the beam relative losses below 10^{-4}. These emittance measurements show a sufficient phase space to accommodate larger emittances when higher intensity heavy-ion beams are accelerated in the FRIB linac. We expect larger than 20% emittance growth for the five-charge-state uranium beam with $\Delta q/q = 6.4\%$, while this value for the three-charge-state xenon beam is 4%.

The poststripper linac was tuned for the $q/A = 50/129 = 0.3876$, which is close to $q/A = 33.5/86 = 0.3895$ and dual-charge-state $^{86}Kr^{33+,34+}$ beam can be accelerated in the LS2 using the same tune developed for $^{129}Xe^{50+}$. The krypton beam energy upstream of the carbon stripper was slightly adjusted to obtain the same energy as $^{129}Xe^{50+}$ downstream of the stripper. The charge selection slits were adjusted for transmission of the krypton beam to the LS2. Because of the lower atomic mass of krypton, the most intense charge state of 34+ contains 60% of the prestripper intensity. Therefore, the acceleration of the dual-charge-state krypton beam provides only a 30% increase in the total intensity. However, by accelerating and delivering the dual-charge-state krypton beam to the production target, the losses and radio activation on the charge selection slits at 17 MeV/nucleon are substantially reduced. The results of

the emittance measurements of the krypton beam are shown in the bottom plots in Fig. 5.

Currently, there is no beam instrumentation available for longitudinal emittance measurements downstream of the stripper. Therefore, the evaluation of the longitudinal phase space after the recombination was performed by the 3D computer simulation with TRACK from the injector to the entrance of 13th cryomodule out of a total 24 in LS2 (see Fig. 2 in Supplemental Material [12] for more details).

Summary.—Simultaneous acceleration of multiple-charge-state beams in the driver linac of the FRIB has been fully established. The trajectories of the bunch centroid x_c, y_c, z_c of each charge state of the xenon beam were measured along the linac with respect to the reference charge state 50+, which was used for the tuning of all focusing, bending, and accelerating components of the linac's poststripper section. The comparison of the measured data with detailed computer simulations using realistic 3D fields shows excellent consistency. For the first time, the recombination of multiple charge states of the same ion species in the 6D phase space is demonstrated. The transmission of the multiple-charge-state beams of xenon and krypton was 100% downstream of the charge selection slits, and no beam losses were detected. The rms emittances were measured for the 180 MeV/nucleon xenon and krypton beams for individual and multiple charge state beams. These measurements showed that the 10σ emittance of the multiple-charge-state beam is well within the acceptance with a significant margin. The results presented in this Letter demonstrate that the simultaneous acceleration of multiple-charge-state heavy-ion beams can be effectively used in the adequately designed high-power heavy-ion linacs.

The authors thank FRIB staff for supporting the linac operation during the experiments with multiple-charge-state beams. The authors appreciate the encouragement and strong support of this work by Professor T. Glasmacher and thank Dr. M. Hausmann for reviewing the manuscript and providing valuable comments. This work is supported by the U.S. Department of Energy Office of Science under Cooperative Agreement No. DE-SC0000661, the State of Michigan, and Michigan State University.

[1] J. Nolen and F. Marti, Charge strippers of heavy ions for high intensity accelerators, Rev. Accel. Sci. Techol. **06**, 221 (2013).

[2] J. Wei *et al.*, The FRIB superconducting Linac—Status and plans, Int. J. Mod. Phys. E **28**, 1930003 (2019).

[3] *Linear Accelerators*, edited by P. M. Lapostolle and A. L. Septier (North-Holland Publishing Company, Holland, 1970).

[4] P. N. Ostroumov, R. C. Pardo, G. P. Zinkann, K. W. Shepard, and J. A. Nolen, Simultaneous Acceleration of Multiply Charged Ions Through a Superconducting Linac, Phys. Rev. Lett. **86**, 2798 (2001).

[5] P. N. Ostroumov and K. W. Shepard, Multiple-charge beam dynamics in an ion linac, Phys. Rev. ST Accel. Beams **3**, 030101 (2000).

[6] Q. Zhao, A. Facco, F. Marti, E. Pozdeyev, M. J. Syphers, J. Wei, X. Wu, Y. Yamazaki, and Y. Zhang, FRIB Accelerator Beam Dynamics Design and Challenges, HB'2012, p. 404, https://accelconf.web.cern.ch/accelconf/HB2012/papers/weo3b01.pdf.

[7] S. Lidia *et al.*, Overview of beam diagnostic systems for FRIB, in *Proceedings of IBIC 2015* (Melbourne, Australia, 2015), p. 226, http://accelconf.web.cern.ch/IBIC2015/papers/mopb071.pdf.

[8] K. L. Brown, F. Rothacker, D. C. Carey, and C. Iselin, TRANSPORT, A computer program for designing charged particle beam transport systems, SLAC-91, Rev. 3, UC-28, 1983.

[9] P. N. Ostroumov, M. Hausmann, K. Fukushima, T. Maruta, A. S. Plastun, M. Portillo, J. Wei, T. Zhang, and Q. Zhao, Heavy ion beam physics at facility for rare isotope beams, J. Instrum. **15**, P12034 (2020).

[10] P. N. Ostroumov, T. Maruta, S. Cogan, K. Fukushima, S. H. Kim, S. Lidia, F. Marti, A. S. Plastun, J. Wei, T. Yoshimoto, T. Zhang, and Q. Zhao, Beam commissioning in the first superconducting segment of the facility for rare isotope beams, Phys. Rev. Accel. Beams **22**, 080101 (2019).

[11] M. G. Minty and F. Zimmermann, *Measurement and Control of Charged Particle Beams* (Springer, New York, 2003).

[12] See Supplemental Material at http://link.aps.org/supplemental/10.1103/PhysRevLett.126.114801 for additional details of the experiment and theoretical modeling.

[13] P. N. Ostroumov, V. N. Aseev, and B. Mustapha, TRACK—A code for beam dynamics simulations in accelerators and transport lines with 3D electric and magnetic fields, 2007, https://www.phy.anl.gov/atlas/TRACK/Trackv39/Manuals/tv39_man_index.html.